

Electron Neutrino Pair Annihilation: A New Source for Muon and Tau Neutrinos in Supernovae

Robert Buras^{1,2}, Hans-Thomas Janka¹, Mathias Th. Keil²,
Georg G. Raffelt², and Markus Rampp¹

¹*Max-Planck-Institut für Astrophysik, Karl-Schwarzschild-Str. 1, 85741 Garching, Germany*

²*Max-Planck-Institut für Physik (Werner-Heisenberg-Institut)
Föhringer Ring 6, 80805 München, Germany*

ABSTRACT

We show that in a supernova core the annihilation process $\nu_e \bar{\nu}_e \rightarrow \nu_{\mu,\tau} \bar{\nu}_{\mu,\tau}$ is always more important than the traditional reaction $e^+ e^- \rightarrow \nu_{\mu,\tau} \bar{\nu}_{\mu,\tau}$ as a source for muon and tau neutrino pairs. We study the impact of the new process by means of a Monte Carlo transport code with a static stellar background model and by means of a self-consistent hydrodynamical simulation with Boltzmann neutrino transport. Nucleon bremsstrahlung $NN \rightarrow NN \nu_{\mu,\tau} \bar{\nu}_{\mu,\tau}$ is also included as another important source term. Taking into account $\nu_e \bar{\nu}_e \rightarrow \nu_{\mu,\tau} \bar{\nu}_{\mu,\tau}$ increases the ν_μ and ν_τ luminosities by as much as 20% while the spectra remain almost unaffected. In our hydrodynamical simulation the shock was somewhat weakened. Elastic $\nu_{\mu,\tau} \nu_e$ and $\nu_{\mu,\tau} \bar{\nu}_e$ scattering is not negligible but less important than $\nu_{\mu,\tau} e^\pm$ scattering. Its influence on the $\nu_{\mu,\tau}$ fluxes and spectra is small after all other processes have been included.

Subject headings: neutrinos — supernovae: general

1. INTRODUCTION

The treatment of ν_μ and ν_τ transport in numerical supernova (SN) simulations has been somewhat schematic in the past. However, with the advent of numerical Boltzmann solvers for the neutrino transport (Mezzacappa & Bruenn 1993, Mezzacappa & Messer 1999; Yamada, Janka, & Suzuki 1999; Burrows et al. 2000; Rampp & Janka 2002) and their application to the post-bounce phase of stellar core-collapse models (Rampp & Janka 2000; Mezzacappa et al. 2001; Liebendörfer et al. 2001) a new level of accuracy has been achieved. Evidently it is desirable that in consistent state-of-the-art simulations the uncertainties are not dominated by overly crude approximations of the microphysics which governs the neutrino interactions. For example, it has been recognized that nuclear many-body correlations (Burrows & Sawyer 1998; Reddy et al. 1999) or weak-magnetism effects in neutrino-nucleon interactions (Vogel & Beacom 1999; Horowitz & Li 2000; Horowitz 2002)

should be included.

Previous simulations used iso-energetic scattering on nucleons $\nu_\mu N \rightarrow N \nu_\mu$ as the main opacity source for ν_μ transport, elastic scattering on electrons and positrons $\nu_\mu e^\pm \rightarrow e^\pm \nu_\mu$ as the main energy-exchange reaction, and $e^+ e^- \rightarrow \nu_\mu \bar{\nu}_\mu$ as the only source term for ν_μ production. (Here and in what follows we use ν_μ symbolically for either ν_μ or ν_τ .) However, it is now generally accepted that nucleon bremsstrahlung $NN \rightarrow NN \nu_\mu \bar{\nu}_\mu$ is important or even dominant as a neutrino source reaction (Suzuki 1991,1993; Hannestad & Raffelt 1998; Thompson, Burrows, & Horvath 2000), and that nucleon recoils have a significant impact on the emerging ν_μ flux spectrum (Janka et al. 1996; Raffelt 2001; Keil, Raffelt, & Janka 2002).

In this paper we show that in addition $\nu_e \bar{\nu}_e \rightarrow \nu_\mu \bar{\nu}_\mu$ and its inverse reaction should be included because this process is always far more important than $e^+ e^- \rightarrow \nu_\mu \bar{\nu}_\mu$ as a neutrino source (Fig. 1). Conversely, $\nu_\mu \nu_e$ and $\nu_\mu \bar{\nu}_e$ scattering turns out to be less important than $\nu_\mu e^\pm$ scattering and thus

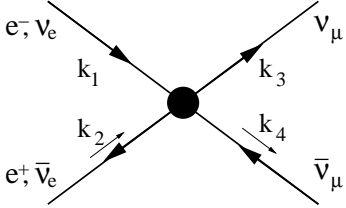


Fig. 1.— Feynman graph for the annihilation processes producing $\nu_\mu\bar{\nu}_\mu$ pairs.

not crucial for the ν_μ flux and spectra formation. Bond (1978) has previously discussed these processes in the context of neutrino transport in supernovae, but no assessment of their relative importance has been performed.

It is straightforward to see that $\nu_e\bar{\nu}_e \rightarrow \nu_\mu\bar{\nu}_\mu$ must be important in a SN core. The region of interest is well inside the ν_μ transport sphere, i.e. interior to the radius where $\nu_\mu N \rightarrow N\nu_\mu$ scattering freezes out. This region is always deeper in the star than the freeze-out radius of the charged-current reactions $\nu_e n \leftrightarrow p e^-$ and $\bar{\nu}_e p \leftrightarrow n e^+$, implying that in the ν_μ trapping region ν_e and $\bar{\nu}_e$ are essentially in local thermodynamic equilibrium (LTE). Therefore, in this region the process $\nu_e\bar{\nu}_e \leftrightarrow \nu_\mu\bar{\nu}_\mu$ will serve to create or destroy $\nu_\mu\bar{\nu}_\mu$ pairs in the same way as the traditional $e^+e^- \leftrightarrow \nu_\mu\bar{\nu}_\mu$ process. With vanishing chemical potentials of e^- and ν_e , the rate of the new process turns out to be about twice that of the traditional one so that the combined source strength would be three times the traditional one.

In the presence of non-vanishing chemical potentials the enhancement is even larger. The pair production rate due to $e^+e^- \rightarrow \nu_\mu\bar{\nu}_\mu$ is shown in Fig. 2 as a function of the degeneracy parameter $\eta_e = \mu_e/T$ for the electrons, and likewise, the rate for $\nu_e\bar{\nu}_e \rightarrow \nu_\mu\bar{\nu}_\mu$ as a function of η_{ν_e} . The production rate is a decreasing function of η . Since in the relevant regions of the SN core $\eta_{\nu_e} < \eta_e$, the traditional process of e^+e^- annihilation is reduced more strongly than the new $\nu_e\bar{\nu}_e$ rate. The latter therefore dominates even more.

In order to estimate the impact of the new source reaction on the neutrino fluxes and spectra we conduct two separate numerical investigations. First, we perform a Monte Carlo transport simulation on a static stellar background model. While this approach has the disadvantage of not follow-

ing the evolution of the neutron star atmosphere self-consistently, it enables us to disentangle the individual effects of different neutrino processes on the transport and spectra formation in a systematic study. Next, we perform two full-scale numerical post-bounce simulations where once the new process is included and once it is left out. This allows us to verify that the effects established by the Monte Carlo results are generic and also show up in self-consistent radiation-hydrodynamical models. The use of these two different approaches and independent codes also helps making sure that our results do not depend on details of the technical implementation or the particular numerical resolution.

We begin in Sec. 2 by comparing the e^+e^- and $\nu_e\bar{\nu}_e$ reactions. In Sec. 3 we discuss the results of a Monte Carlo study of neutrino transport while in Sec. 4 we describe the self-consistent hydrodynamical simulations coupled with a Boltzmann transport solver. We summarize our findings in Sec. 5.

2. ELECTRON VS. NEUTRINO PAIR ANNIHILATION

We begin by comparing the two pair annihilation processes

$$\nu_e + \bar{\nu}_e \rightarrow \nu_\mu + \bar{\nu}_\mu, \quad (1)$$

$$e^+ + e^- \rightarrow \nu_\mu + \bar{\nu}_\mu. \quad (2)$$

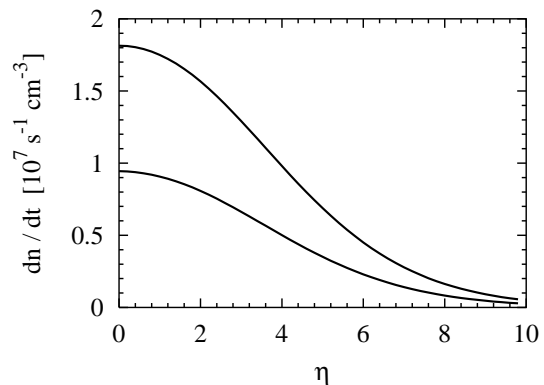


Fig. 2.— Pair production rates by the process $\nu_e\bar{\nu}_e \rightarrow \nu_\mu\bar{\nu}_\mu$ as a function of η_{ν_e} (upper line) and $e^+e^- \rightarrow \nu_\mu\bar{\nu}_\mu$ as a function of η_e (lower line). We used $T = 12$ MeV and $\eta_{\nu_\mu} = 0$.

TABLE 1
WEAK INTERACTION CONSTANTS.

Process:	$e^+e^- \leftrightarrow \nu_\mu\bar{\nu}_\mu$	$\nu_e\bar{\nu}_e \leftrightarrow \nu_\mu\bar{\nu}_\mu$
C_V	$-\frac{1}{2} + 2\sin^2\theta_w$	$+\frac{1}{2}$
C_A	$-\frac{1}{2}$	$+\frac{1}{2}$

In the relativistic limit where the electron mass can be neglected, their squared and spin-summed matrix elements are of the form

$$\sum_{\text{spins}} |\mathcal{M}|^2 = 8 G_F^2 [(C_V + C_A)^2 u^2 + (C_V - C_A)^2 t^2], \quad (3)$$

with the Mandelstam variables $t = -2k_1 \cdot k_3$ and $u = -2k_1 \cdot k_4$. The momenta are assigned to the particles as indicated in Fig. 1. The matrix elements for the two processes differ only in the weak coupling constants $C_{V,A}$ shown in Table 1.

The pair production rate is obtained by appropriate phase-space integrations, including particle distributions and blocking factors (Yueh & Buchler 1976; Hannestad & Madsen 1995). We use $\mu_{\nu_\mu} = 0$ even though there could be a small ν_μ chemical potential due to a non-vanishing concentration of muons in the core and due to different transport properties of ν_μ and $\bar{\nu}_\mu$. Assuming that e^\pm , ν_e , and $\bar{\nu}_e$ are all in LTE, the rates of pair creation vs. degeneracy parameters η_e and η_{ν_e} are shown in Fig. 2. In the dense regions of a SN core below the neutrino spheres the phase space distribution of electron neutrinos is a Fermi-Dirac function with degeneracy parameter $\eta_{\nu_e} = \eta_e + \eta_p - \eta_n < \eta_e$ so that the new process is always more important than e^+e^- annihilation.

An interesting difference between the two processes arises in the differential production rates, i.e. the ν_μ and $\bar{\nu}_\mu$ production rates as functions of neutrino energy ϵ . As a first case we take $\eta = 0$ for both e and ν_e and show the differential production rate $d^2n/d\epsilon dt$ in Fig. 3. For both processes the differential rate is the same for ν_μ and $\bar{\nu}_\mu$, i.e. they are produced with the same spectra.

However, in general the ‘‘parent particles’’ will have a significant chemical potential. Taking $\eta_e =$

$\eta_{\nu_e} = 10$ we show the differential production rates in Fig. 4. In case of the e^+e^- process (upper panel) the differential rates are similar for ν_μ and $\bar{\nu}_\mu$. This is understood by the fact that the values of $(C_V + C_A)^2 \simeq 0.54^2$ and $(C_V - C_A)^2 \simeq 0.46^2$ are quite similar so that the u^2 and t^2 terms in Eq. (3) are almost equally important. Therefore, interchanging ν_μ and $\bar{\nu}_\mu$, corresponding to an exchange of u and t , has no big effect.

This is not true for the neutrino reaction, where $(C_V + C_A)^2 = 1$ and $(C_V - C_A)^2 = 0$ and thus only u^2 contributes. Replacing u by t now changes the kinematics of the process, which in turn modifies the rate if the distribution of ν_e differs from that of $\bar{\nu}_e$, i.e. if $\eta_{\nu_e} \neq 0$. The ν_μ and $\bar{\nu}_\mu$ spectra shown in the bottom panel of Fig. 4 are indeed very different from each other, although the total production rates of ν_μ and $\bar{\nu}_\mu$ are, of course, equal.

One can easily understand why ν_μ on average have larger energies than $\bar{\nu}_\mu$. We first look at $\nu_e\bar{\nu}_e \rightarrow \nu_\mu\bar{\nu}_\mu$ in the center of momentum (CM)

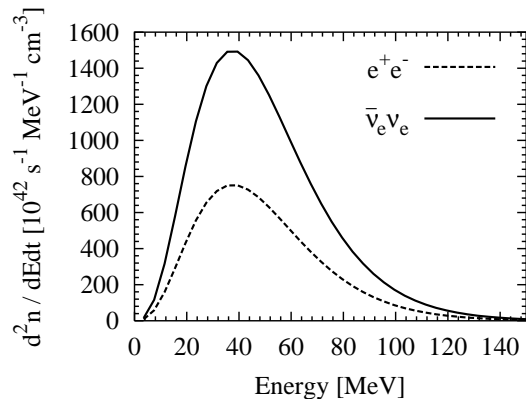


Fig. 3.— Differential ν_μ and $\bar{\nu}_\mu$ production rates $d^2n/d\epsilon dt$ vs. neutrino energy for $\eta_e = \eta_{\nu_e} = 0$ and $T = 12$ MeV.

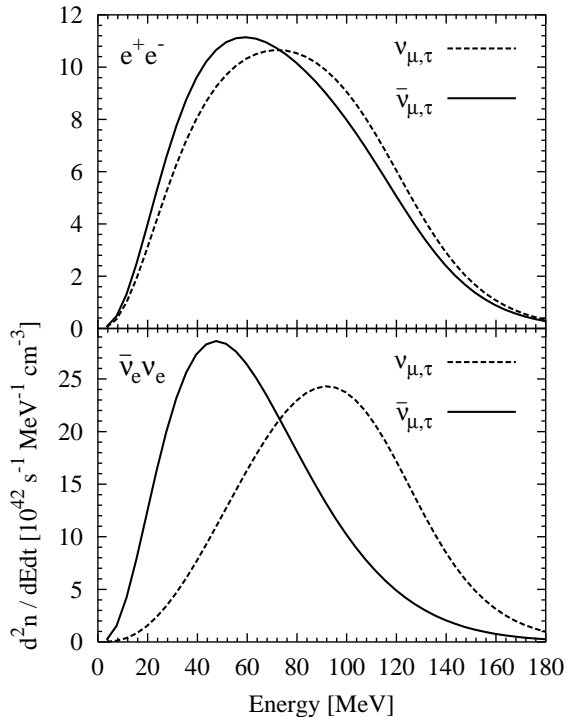


Fig. 4.— Differential ν_μ and $\bar{\nu}_\mu$ production rates $d^2n/dedt$ for $\eta_e = \eta_{\nu_e} = 10$ and $T = 12$ MeV. Upper panel for $e^+e^- \rightarrow \nu_\mu\bar{\nu}_\mu$, lower panel for $\nu_e\bar{\nu}_e \rightarrow \nu_\mu\bar{\nu}_\mu$.

frame. The differential cross section is

$$\frac{d\sigma}{d\cos\theta} = \frac{G_F^2}{4\pi} \epsilon^2 (1 + \cos\theta)^2, \quad (4)$$

where θ is the angle between the ingoing ν_e and the outgoing ν_μ , or equivalently, between the ingoing $\bar{\nu}_e$ and the outgoing $\bar{\nu}_\mu$. Put another way, forward scattering is favored and backward scattering forbidden. This is due to angular momentum conservation. The ingoing ν_e and $\bar{\nu}_e$ have opposite helicities and, in the CM frame, opposite momenta, so that their combined spins add up to 1. The same is true for the outgoing particles so that backward scattering would violate angular momentum conservation. In the rest frame of the medium the ingoing ν_e tends to have energies of the order of its Fermi energy, while the ingoing $\bar{\nu}_e$ tends to have energies of order T . Because forward scattering is favored, the outgoing ν_μ tends to inherit the larger energy of the ingoing ν_e .

The differences of the source spectra, however,

do not translate into significant spectral differences of the ν_μ and $\bar{\nu}_\mu$ fluxes emitted from the SN core. While pair annihilations and nucleon bremsstrahlung are responsible for producing or absorbing neutrino pairs and thus their equilibration with the stellar medium below the “neutrino-energy sphere,” other processes, notably $\nu_\mu e^\pm$ scattering and nucleon recoils, are more efficient for the exchange of energy between neutrinos and the medium between the equilibration and transport spheres. In our numerical runs we will find in fact that adding the new process to a SN simulation primarily modifies the flux with only minor modifications of the spectrum.

If $\nu_e\bar{\nu}_e \rightarrow \nu_\mu\bar{\nu}_\mu$ is important relative to $e^+e^- \rightarrow \nu_\mu\bar{\nu}_\mu$ one may wonder if processes of the form

$$\nu_\mu + \nu_e \rightarrow \nu_\mu + \nu_e, \quad (5)$$

$$\nu_\mu + \bar{\nu}_e \rightarrow \nu_\mu + \bar{\nu}_e, \quad (6)$$

could be of comparable importance as $\nu_\mu e^\pm$ scattering. Figure 5 shows the rates for ν_μ scattering on ν_e and $\bar{\nu}_e$, and those for scattering on e^+ and e^- as functions of η_{ν_e} and η_e , respectively. The rates are normalized to the $\nu_\mu e^\pm$ rate at $\eta_e = 0$. In contrast to the annihilation rates, the scattering rates rise monotonically with η . Therefore, even though neutrino-neutrino scattering would dominate if all chemical potentials were zero, for realistic situations with $\eta_{\nu_e} < \eta_e$ we expect that scattering on e^\pm has 1–2 times the rate of scattering on

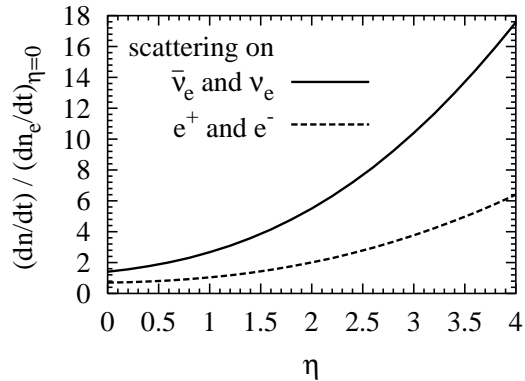


Fig. 5.— Thermally averaged scattering rate for ν_μ on e^\pm as a function of η_e (lower line) and for ν_μ on ν_e and $\bar{\nu}_e$ (upper line) as a function of η_{ν_e} . The rates are normalized to the scattering rate on e^\pm at $\eta_e = 0$. We used $T = 12$ MeV and $\eta_{\nu_\mu} = 0$.

ν_e and $\bar{\nu}_e$. Therefore, neutrino-neutrino scattering is expected to be a relatively minor correction. In our Monte Carlo studies we will indeed find that this process has only a small effect on the neutrino spectra and fluxes.

3. MONTE CARLO STUDY

To study the impact of the new annihilation process on the ν_μ fluxes and spectra we first use a Monte Carlo method for neutrino transport on a static background stellar model. For this purpose we have adapted the Monte Carlo code of Janka & Hillebrandt (1989a,b) to include additional processes and nucleon recoil. We use this code for an extensive parameter study of ν_μ spectra formation that will be documented elsewhere (Keil et. al. 2002).

As a stellar background we employ a model originally provided to us by B. Messer for an earlier study of neutrino spectra formation (Raffelt 2001). Using this model again for our present study facilitates a comparison with this previous work. The model is based on a full-scale Newtonian collapse simulation of the Woosley & Weaver $15 M_\odot$ progenitor model labeled s15s7b. We use a snapshot at 324 ms after bounce when the shock wave is at a radius of about 120 km, i.e. the SN core still accretes matter. In Fig. 6 the temperature profile is represented by the steps in terms of $\langle\epsilon\rangle \simeq 3.15 T$ for each radial zone, i.e. by the average energy of nondegenerate neutrinos ($\eta_{\nu_\mu} = 0$) in LTE with the stellar medium.

In Fig. 6 we also show the thermalization depth R_{therm} for several processes as a function of neutrino energy ϵ . The formal definition of R_{therm} in terms of an effective mean free path for energy exchange is given by the condition (cf. Shapiro & Teukolsky 1983; Suzuki 1989; Raffelt 2001)

$$\tau_{\text{eff}}(\epsilon) = \int_{R_{\text{therm}}}^{\infty} dr \sqrt{\frac{1}{\lambda_i} \sum_j \frac{1}{\lambda_j}} = \frac{2}{3} \quad (7)$$

for the effective optical depth τ_{eff} of a particular equilibrating process with mean free path $\lambda_i(\epsilon)$ among the opacity producing reactions having mean free paths $\lambda_j(\epsilon)$. The solid line in Fig. 6 is for $\nu_e n \rightarrow p e^-$, i.e. it represents the energy-dependent ν_e sphere. The dashed line is the analogous $\bar{\nu}_e$ sphere due to $\bar{\nu}_e p \rightarrow n e^+$. Finally, the dot-

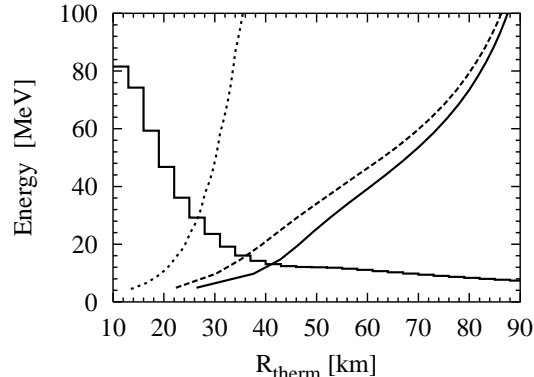


Fig. 6.— Thermalization depth R_{therm} (horizontal axis) for different processes as a function of neutrino energy ϵ (vertical axis) in our background model. The energy-exchanging processes are $\nu_e n \rightarrow p e^-$ (solid line), $\bar{\nu}_e p \rightarrow n e^+$ (dashed line), and $\nu_\mu \bar{\nu}_\mu$ annihilation to $\nu_e \bar{\nu}_e$ pairs (dotted line). The steps represent the temperature profile of the stellar model in terms of $\langle\epsilon\rangle \simeq 3.15 T$.

ted line shows where ν_μ or $\bar{\nu}_\mu$ of given energy last participate in the $\nu_\mu \bar{\nu}_\mu \rightarrow \nu_e \bar{\nu}_e$ process, assuming that the annihilation partners are distributed according to LTE. Put another way, the dotted line is the energy-dependent freeze-out sphere for our new process. It is always at much smaller radii than the ν_e and $\bar{\nu}_e$ spheres. Therefore, in those regions where $\nu_\mu \bar{\nu}_\mu \leftrightarrow \nu_e \bar{\nu}_e$ is effective we may assume LTE for ν_e and $\bar{\nu}_e$.

We therefore implemented the new process in our Monte Carlo code by using the same subroutine as for the e^+e^- pair process, except for inserting the appropriate weak interaction constants $C_{V,A}$ and replacing η_e by η_{ν_e} .

We summarize the characteristics of the emerging neutrino flux for our runs in Table 2. As introduced by Janka & Hillebrandt (1989a) we characterize the neutrino spectrum by its first two energy moments $\langle\epsilon\rangle_{\text{flux}}$ and $\langle\epsilon^2\rangle_{\text{flux}}$ and define the “pinching parameter” by following Raffelt (2001) as

$$p_{\text{flux}} \equiv \frac{1}{a} \frac{\langle\epsilon^2\rangle_{\text{flux}}}{\langle\epsilon\rangle_{\text{flux}}^2}, \quad (8)$$

with the energy moments

$$\langle\epsilon^n\rangle_{\text{flux}} = \frac{\int_0^\infty d\epsilon \int_{-1}^{+1} d\mu f_\nu(\epsilon, \mu) \epsilon^{n+2} \mu}{\int_0^\infty d\epsilon \int_{-1}^{+1} d\mu f_\nu(\epsilon, \mu) \epsilon^2 \mu} \quad (9)$$

TABLE 2
SPECTRAL CHARACTERISTICS OF NEUTRINO FLUXES FROM MONTE CARLO TRANSPORT.

Energy exchange	$\langle\epsilon\rangle_{\text{flux}}$ [MeV]	$\langle\epsilon^2\rangle_{\text{flux}}$ [MeV ²]	p_{flux}	T [MeV]	η	L_ν [10 ⁵¹ $\frac{\text{erg}}{\text{s}}$]
ν_μ transport						
original run	17.5	388.	0.97	5.2	1.1	14.4
– – s p –	16.6	362.	1.01	5.3	–0.3	15.8
– – s p n	16.9	369.	0.99	5.3	0.4	20.2
b r s p –	14.2	255.	0.98	4.2	1.1	14.8
b r s p n	14.4	264.	0.97	4.3	1.2	17.6
b r s – n	14.4	263.	0.97	4.3	1.2	17.0
b r sn p n	14.3	260.	0.97	4.3	1.2	17.9
$\bar{\nu}_\mu$ transport						
– – s p n	16.9	368.	0.99	5.2	0.6	20.6
b r s p n	14.4	263.	0.97	4.2	1.3	17.8
b r s – n	14.4	262.	0.98	4.3	1.1	16.8

NOTE.—For energy exchange, “b” refers to bremsstrahlung, “r” to recoil, “s” to scattering on electrons and positrons, “p” to e^+e^- pair annihilation, “n” to $\nu_e\bar{\nu}_e$ pair annihilation, and “sn” to scattering on both, e^\pm and $\nu_e, \bar{\nu}_e$.

of the emergent flux spectrum. Here $f_\nu(\epsilon, \mu)$ is the neutrino distribution function in energy-angle space with μ being the cosine of the angle of neutrino propagation relative to the radial direction. The constant a for a Fermi-Dirac distribution at zero chemical potential is

$$a \equiv \frac{\langle \epsilon^2 \rangle}{\langle \epsilon \rangle^2} = \frac{486000 \zeta_3 \zeta_5}{49 \pi^8} \approx 1.3029. \quad (10)$$

Then $p = 1$ signifies that the spectrum is thermal up to its second moment, while $p < 1$ signifies a pinched spectrum (high-energy tail suppressed), and $p > 1$ an anti-pinched spectrum (high-energy tail enhanced). For $p < 1.023$ it is common to approximate the spectrum as a nominal Fermi-Dirac distribution characterized by a temperature T and a degeneracy parameter η which are chosen such that $\langle \epsilon \rangle_{\text{flux}}$ and $\langle \epsilon^2 \rangle_{\text{flux}}$ are reproduced (Table 2). Finally we show the neutrino luminosity in the last column of Table 2.

We always include elastic $\nu_\mu N$ scattering which provides the dominant opacity contribution. In a given run we additionally include those energy-exchanging processes which are indicated in the first columns of Table 2. We use “b” to indicate bremsstrahlung $NN \rightarrow NN\nu_\mu\bar{\nu}_\mu$, “r” for recoil in $\nu_\mu N \rightarrow N\nu_\mu$, “s” for $\nu_\mu e^\pm$ scattering, “p” for the traditional pair annihilation process $e^+e^- \rightarrow \nu_\mu\bar{\nu}_\mu$, “n” for the new neutrino annihilation process $\nu_e\bar{\nu}_e \rightarrow \nu_\mu\bar{\nu}_\mu$, and “sn” for $\nu_\mu e^\pm$ plus $\nu_\mu\nu_e$ and $\nu_\mu\bar{\nu}_e$ scattering.

In the first row of Table 2 we show the original flux characteristics of our background model from the calculation of Messer et al. (2002). Running our code with the same neutrino reactions—scattering on e^\pm (s) and e^+e^- pair annihilation (p)—we find the results in the second row. We attribute the small differences to the different numerical approaches. In particular, the Boltzmann solver of Messer et al. (2002) works in practice with a limited number of energy bins. Moreover, there may be differences in the implementation of the microphysical reactions. Finally, in the Monte Carlo code we assume that neutrinos are in thermodynamic equilibrium with the stellar medium at the inner boundary. This choice of boundary condition may have a small effect on our results since the thermalization depth of e^+e^- pair processes is strongly energy dependent and thus low energy ν_μ are forced into equilibrium by our

boundary condition instead of the pair process. We interpret the first two rows of Table 2 as agreeing satisfactorily well with each other.

Next we add $\nu_e\bar{\nu}_e$ annihilation (n). The spectrum remains almost unchanged, but the luminosity increases by about 30%. Therefore, the new process has a rather significant impact on the predicted ν_μ luminosity.

However, other processes are also important which in the past have not been included in numerical simulations. Therefore, we switch off the new process and instead include bremsstrahlung (b) and recoil (r). Compared to the original run we obtain almost the same luminosity, but significantly lowered spectral energies. Now we again include $\nu_e\bar{\nu}_e$ annihilation (n) and find that the spectra remain unaffected, but the luminosity increases by about 20%. Therefore, even with all other energy-exchanging reactions included, the $\nu_e\bar{\nu}_e$ process still has an important effect on the luminosity. We finally switch off the traditional pair process (p), but keep the new one. The spectra remain unaffected, the luminosity slightly drops. It is evident that the $\nu_e\bar{\nu}_e$ process is by far the dominant leptonic source reaction for muon neutrinos. Its importance relative to bremsstrahlung will depend sensitively on the background model (Keil et. al. 2002).

As a last step we include the scattering on ν_e and $\bar{\nu}_e$ in addition to all other processes. The rate for this process is typically half as large as the rate for scattering on e^\pm , in agreement with Fig. 5 if we use $\eta_e \simeq 3$ and $\eta_{\nu_e} \simeq 0.3$. The effect on the ν_μ flux and spectrum is minimal and in fact below the numerical resolution of our Monte Carlo runs.

In the second part of Table 2 we finally show several runs for the transport of anti-neutrinos. Recall that $\nu_e\bar{\nu}_e \rightarrow \nu_\mu\bar{\nu}_\mu$ generates different source spectra for ν_μ and $\bar{\nu}_\mu$. Of course, the small differences between ν_μ and $\bar{\nu}_\mu$ scattering off electrons and positrons are also taken into account, as well as the small differences in e^+e^- pair annihilation. Comparing the $\bar{\nu}_\mu$ runs with those for ν_μ we find excellent agreement. Therefore, the detailed spectral distribution of the pair rate is not important, only the total rate of absorption and production of $\nu_\mu\bar{\nu}_\mu$ pairs matters.

4. HYDRODYNAMICAL SIMULATION WITH BOLTZMANN TRANSPORT

The large flux increase found by the Monte Carlo method may not persist in a self-consistent hydrodynamical treatment where the stellar model can adjust in response to the modified transport. For this reason we have performed a Boltzmann transport simulation coupled with a full hydrodynamics code (Rampp & Janka 2002) for the $15 M_{\odot}$ progenitor model s15s7b2 (Woosley, personal communication; Woosley & Weaver 1995).

In order to minimize the required modifications of the code we treat the transport of ν_{μ} and $\bar{\nu}_{\mu}$ identically. Therefore, we use an average source strength for the ν_{μ} and $\bar{\nu}_{\mu}$ production from $\nu_e\bar{\nu}_e$ annihilation, ignoring the spectral differences. The Monte Carlo results suggest that this approximation is well justified.

For computing the interaction rates we again assume LTE for ν_e and $\bar{\nu}_e$ in all regions where the new annihilation process is important. This assumption also justifies introducing an energy source term for the new process directly into the medium energy equation in perfect analogy to the source term of the process $e^+e^- \leftrightarrow \nu\bar{\nu}$. Similarly, the scattering reactions of ν_{μ} and $\bar{\nu}_{\mu}$ off ν_e and $\bar{\nu}_e$ can be treated in full correspondence to the scattering off electrons and positrons by a simple change of the weak coupling coefficients. Thus a direct coupling of the ν_{μ} and ν_e sectors of the neutrino transport code is avoided. For the new process this is achieved only indirectly via the stellar medium as an intermediary.

Our baseline for comparison is a Newtonian simulation which includes the transport of neutrinos of all three flavors. Neutrino-medium interactions for all relevant processes are implemented, notably nucleon bremsstrahlung, as described by Rampp & Janka (2002). Note, however, that nucleon recoils are not taken into account in the results shown for the baseline simulation (thin lines in Figs. 7, 8 and 9). Rather, the charged-current and neutral-current neutrino reactions with nucleons are handled in the “old standard approximation” of infinitely massive nucleons at rest following the treatment by Bruenn (1985) and Mezzacappa & Bruenn (1993).

In a second simulation we included the new leptonic process for $\nu_{\mu}\bar{\nu}_{\mu}$ pair production and anni-

hilation. The results for this run are depicted as thick lines in the figures. In Figs. 7 and 8 we show the evolution of the neutrino luminosities and of the root mean squared (rms) energies as functions of time after bounce. The rms energy is defined in the usual way (e.g. Messer et al. 1998) by

$$\langle\epsilon\rangle_{\text{rms}} = \sqrt{\frac{\int_0^{\infty} d\epsilon \int_{-1}^{+1} d\mu f_{\nu}(\epsilon, \mu) \epsilon^5}{\int_0^{\infty} d\epsilon \int_{-1}^{+1} d\mu f_{\nu}(\epsilon, \mu) \epsilon^3}}, \quad (11)$$

i.e. using the neutrino energy distribution as a weight function. The results are given for an observer who is comoving with the stellar fluid at a radial location of 500 km. The Doppler-blueshift due to the infall velocity of the matter is rather small at this distance from the neutrino emitting neutron star so that the quantities are close to the observable properties at infinity.

As expected, the ν_{μ} luminosity is increased by 10–20%, but the spectrum remains essentially unaffected. The enhanced energy loss leads to a somewhat faster proto-neutron star contraction. This causes small changes also in the region where the electron neutrino and antineutrino fluxes are built up and where these neutrinos finally decouple from the stellar background. As a consequence, the mean spectral energies of ν_e and $\bar{\nu}_e$ are systematically higher by a small amount (Fig. 8). Initially, the ν_e luminosity is also slightly larger (Fig. 7) but after about 150 ms post bounce the luminosities of ν_e and $\bar{\nu}_e$ drop below the level of those in the reference simulation. This is caused by the decrease of the radii of the neutrino spheres in response to the accelerated contraction of the proto-neutron star. At 200 ms after bounce the $\nu_{\mu,\tau}$ luminosities of the two models then become nearly equal, probably as a consequence of two competing effects which seem to essentially compensate each other at later times: On the one hand side the neutrino emission of the nascent neutron star decays faster with time when the new process is included (as visible from the ν_e and $\bar{\nu}_e$ luminosities), on the other hand the new process raises the energy loss in $\nu_{\mu,\tau}$ compared to ν_e and $\bar{\nu}_e$.

The shock positions in both simulations evolve identically until about 100 ms after bounce. Then the shock is somewhat weakened by introducing the new reaction and expands only to a maximum radius of 230 km instead of 250 km (Fig. 9). This can be understood again by the more com-

compact proto-neutron star, which causes higher infall velocities in the region of heating by ν_e and $\bar{\nu}_e$ absorption behind the shock. This reduces the integral energy deposition by neutrinos as well as the pressure behind the shock front.

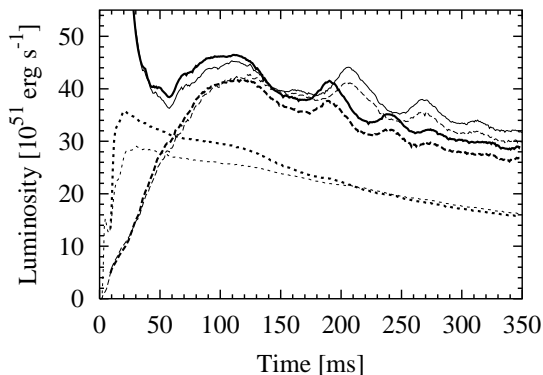


Fig. 7.— Evolution of the luminosities for ν_e (solid), $\bar{\nu}_e$ (dashed) and ν_μ (dotted) as functions of time after bounce for two hydrodynamical simulations with three-flavor Boltzmann neutrino transport. Thick lines represent results of a model with the new process included, thin lines of a reference calculation without this process. The luminosities are measured by an observer comoving with the stellar fluid at 500 km.

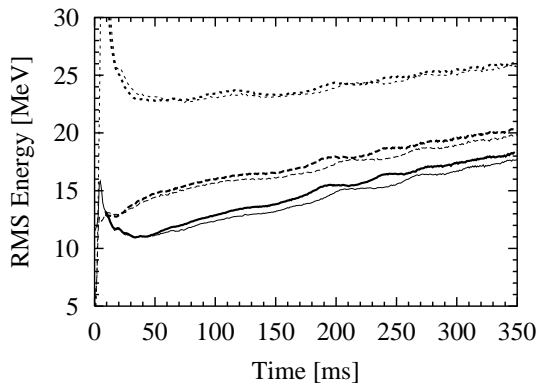


Fig. 8.— Evolution of the rms energies for ν_e (solid), $\bar{\nu}_e$ (dashed) and ν_μ (dotted) as measured by an observer comoving with the stellar fluid at 500 km.

Since we completed this study we have implemented the neutrino annihilation process in simulations with an approximate treatment of general

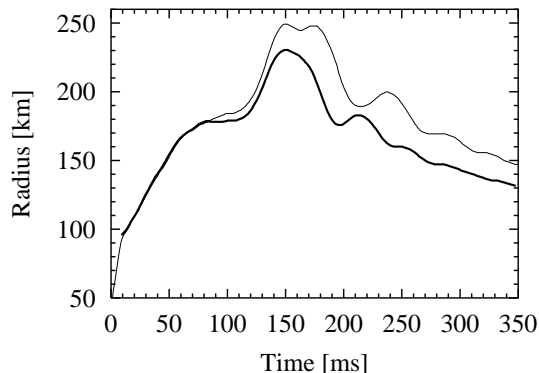


Fig. 9.— Evolution of the shock positions.

relativity (Rampp & Janka 2002). In these new simulations neutrino-nucleon interactions are implemented in terms of dynamical structure functions for correlated nuclear matter and also include weak magnetism corrections (Rampp et al. 2002). Put another way, these simulations include nuclear recoil as well as nuclear correlation effects. The impact of the new process in these more complete simulations is comparable to what we have found here.

5. CONCLUSIONS

We have shown that $\nu_e\bar{\nu}_e$ annihilation is the dominant leptonic source for $\nu_{\mu,\tau}\bar{\nu}_{\mu,\tau}$ pairs in a SN core, far more important than the traditional e^+e^- pair annihilation. Its importance relative to the nucleon bremsstrahlung process, which also has not been included in previous SN simulations, depends on the stellar profile. In our Monte Carlo studies with a background model representing the SN core during the accretion phase, the new process enhanced the ν_μ luminosity by about 20% in a calculation where nucleon bremsstrahlung and energy exchange by nucleon recoils were taken into account. Without these other new effects, $\nu_e\bar{\nu}_e$ annihilation has an even larger impact.

In self-consistent hydrodynamical simulations with Boltzmann neutrino transport we find that during the first 150 ms the effect is similar to that obtained in the static Monte Carlo simulations and has a noticeable influence on the stellar evolution and structure. Later, the ν_μ and $\bar{\nu}_\mu$ luminosities approach those of the model without the new process.

cess of $\nu_e\bar{\nu}_e$ annihilation. At that time, however, the ν_e and $\bar{\nu}_e$ luminosities are smaller. Throughout the simulation the new reaction therefore works in the direction of making the ν_e and $\bar{\nu}_e$ luminosities more similar to those of ν_μ and $\bar{\nu}_\mu$. In the model with the new process the shock is somewhat weakened and reaches only smaller radii.

In all of our Monte Carlo and hydrodynamical runs we confirm the naive expectation that the effect of the new pair production and annihilation process on the neutrino spectra is minimal. The crossed process of $\nu_{\mu,\tau}$ scattering off ν_e and $\bar{\nu}_e$ also turned out to have a negligible impact on the emitted spectra.

We conclude that state-of-the-art SN simulations should include the $\nu_e\bar{\nu}_e$ annihilation reaction to $\nu_{\mu,\tau}\bar{\nu}_{\mu,\tau}$ pairs. While the effects of this process on the neutrino luminosities and spectra and on the shock propagation are not dramatic, they are nevertheless noticeable and not negligible, even after nucleon bremsstrahlung and nucleon recoils have been included. Implementing the new process is not more difficult and not more CPU-expensive than the traditional e^+e^- process.

ACKNOWLEDGEMENTS

We thank Bronson Messer for making the unpublished results of a collapse simulation available. This work was partly funded by the Deutsche Forschungsgemeinschaft under grant No. SFB 375 and the ESF network Neutrino Astrophysics. The radiation-hydrodynamical computations were performed on the NEC SX-5/3C of the Rechenzentrum Garching and the CRAY T90 of the John von Neumann Institute for Computing (NIC) in Jülich, Germany.

REFERENCES

Bond, J. R. 1978, “Neutrino production and transport during gravitational collapse,” (Ph.D. Thesis, California Institute of Technology, Pasadena, California).

Bruenn, S. W. 1985, “Stellar core collapse — Numerical model and infall epoch,” *Ap. J. Suppl.*, 58, 771.

Burrows, A., Young, T., Pinto, P., Eastman, R., & Thompson, T.A. 2000, “A new algorithm for

supernova neutrino transport and some applications,” *Ap. J.*, 539, 865.

Burrows, A., & Sawyer, R.F. 1998, “The effects of correlations on neutrino opacities in nuclear matter,” *Phys. Rev. C*, 58, 554.

Hannestad, S., & Madsen, J. 1995 “Neutrino decoupling in the early universe,” *Phys. Rev. D*, 52, 1764

Hannestad, S., & Raffelt, G. 1998, “Supernova neutrino opacity from nucleon nucleon bremsstrahlung and related processes,” *Ap. J.*, 507, 339.

Horowitz, C. J., & Li, G. 2000, “Charge-conjugation violating neutrino interactions in supernovae,” *Phys. Rev. D*, 61, 063002.

Horowitz, C. J. 2002, “Weak magnetism for antineutrinos in supernovae,” *Phys. Rev. D*, 65, 043001.

Janka, H.-T., & Hillebrandt, W. 1989a, “Neutrino emission from type II supernovae—an analysis of the spectra,” *Astron. Astrophys.*, 224, 49

Janka, H.-T., & Hillebrandt, W. 1989b, “Monte Carlo simulations of neutrino transport in type II supernovae,” *Astron. Astrophys. Suppl. Ser.*, 78, 375

Janka, H.-T., Keil, W., Raffelt, G., & Seckel, D. 1996, “Nucleon spin fluctuations and the supernova emission of neutrinos and axions,” *Phys. Rev. Lett.*, 76, 2621.

Keil, M. Th., Raffelt, G. G., & Janka, H.-T. 2002 “Monte Carlo study of supernova neutrino spectra formation,” (in preparation).

Liebrandt, M., Mezzacappa, A., Thielemann, F., Messer, O. E., Hix, W. R., Bruenn, S. W. 2001, “Probing the gravitational well: No supernova explosion in spherical symmetry with general relativistic Boltzmann neutrino transport,” *Phys. Rev. D*, 63, 3004.

Messer, O. E. B., Mezzacappa, A., Bruenn, S. W., and Guidry, M. W. 1998, “A comparison of Boltzmann and multi-group flux-limited diffusion neutrino transport during the post bounce shock reheating phase in core-collapse supernovae,” *Ap. J.*, 507, 353

- Messer, O. E. B., Mezzacappa, A., Liebendörfer, M., Hix, W. R., Thielemann, F.-K., & Bruenn, S. W. 2002, (in preparation)
- Mezzacappa, A., Bruenn, S. W., 1993, “Type II supernovae and Boltzmann neutrino transport — The infall phase,” *Ap. J.*, 405, 637.
- Mezzacappa, A., Messer, O. E., “Neutrino transport in core collapse supernovae,” 1999, *Journal of Computational and Applied Mathematics*, 109, 281.
- Mezzacappa, A., Liebendörfer, M., Messer, O. E., Hix, W. R., Thielemann, F.-K., & Bruenn, S. W. 2001, “The simulation of a spherically symmetric supernova of a 13 solar mass star with boltzmann neutrino transport, and its implications for the supernova mechanism,” *Phys. Rev. Lett.*, 86, 1935.
- Raffelt, G. G. 2001, “Mu- and tau-neutrino spectra formation in supernovae,” *Ap. J.*, 561, 890.
- Rampp, M., & Janka, H.-T. 2000, “Spherically symmetric simulation with Boltzmann neutrino transport of core collapse and post-bounce evolution of a 15 solar mass star,” *Ap. J.*, 539, L33.
- Rampp, M., & Janka, H.-T. 2002, “Radiation hydrodynamics with neutrinos: Variable Eddington factor method for core-collapse supernova simulations,” *astro-ph/0203101*.
- Rampp, M., Janka, H.-T., Buras, R., Horowitz, C.J. & Takahashi, K. 2002, (in preparation).
- Reddy, S., Prakash, M., Lattimer, J.M., & Pons, J.A. 1999, “Effects of strong and electromagnetic correlations on neutrino interactions in dense matter,” *Phys. Rev. C*, 59, 2888.
- Shapiro, S.L., & Teukolsky, S.A. 1983, “Black holes, white dwarfs and neutron stars: The physics of compact objects,” (John Wiley & Sons, New York).
- Suzuki, H. 1989, “Neutrino burst from supernova explosion and proto neutron star cooling,” (Ph.D. Thesis, University of Tokyo).
- Suzuki, H. 1991, “Neutrino emission from protoneutron star with modified Urca and nucleon bremsstrahlung processes,” *Num. Astrophys. Japan*, 2, 267.
- Suzuki, H. 1993, “Supernova neutrinos—Multi-group simulations of neutrinos from protoneutron star,” in: *Proc. International Symposium on Neutrino Astrophysics: Frontiers of Neutrino Astrophysics, 19–22 Oct. 1992, Takayama, Japan*, edited by Y. Suzuki and K. Nakamura (Universal Academy Press, Tokyo).
- Thompson, T. A., Burrows, A., & Horvath, J. E. 2000, “Muon and tau neutrino thermalization and production in supernovae: Processes and timescales,” *Phys. Rev. C*, 62, 035802.
- Vogel, P., Beacom, J. F., 1999, “Angular distribution of neutron inverse beta decay, $\bar{\nu}_e + p \rightarrow e^+ + n$,” *Phys. Rev. D*, 60, 053003.
- Woolsey, S. E. & Weaver, T. A. 1995, “The evolution and explosion of massive stars. II. Explosive hydrodynamics and nucleosynthesis,” *Ap. J. Suppl.*, 101, 181.
- Yamada, S., Janka, H.-Th., Suzuki, H., 1999, “Neutrino transport in type II supernovae: Boltzmann solver vs. Monte Carlo method,” *Astron. Astrophys.*, 344, 533.
- Yueh, W. R., & Buchler, J. R. 1976, “Scattering functions for neutrino transport,” *Astrophys. Space Sci.*, 39, 429.